Design of coupling parameters for inducing amplitude death in Cartesian product networks of delayed coupled oscillators

Design of coupling parameters for inducing amplitude death in Cartesian product networks of delayed coupled oscillators

Yoshiki Sugitani[1] and Keiji Konishi[2]

[1]*Department of Electrical and Electronic Engineering, Ibaraki University 4-12-1 Nakanarusawa, Hitachi, Ibaraki 316-8511, Japan*
[2]*Department of Electrical and Information Systems, Osaka Prefecture University, 1-1 Gakuen-cho, Naka-ku, Sakai, Osaka 599-8531, Japan*

The present study investigates amplitude death in Cartesian product networks of two subnetworks, where each subnetwork has a different coupling delay. The property of the Cartesian product helps us to analyze the stability of amplitude death. Our analysis reveals that amplitude death can occur for long coupling delays if there is a suitable difference in the coupling delays in the two subnetworks. Furthermore, based on the edge theorem in robust control theory, we propose two design procedures of coupling parameters for inducing amplitude death in the Cartesian product networks. Our procedures do not require any information of topologies of the subnetworks. The validity of these procedures is numerically confirmed.

I. INTRODUCTION

Nonlinear phenomena in coupled oscillators are an active field of research [1,2]. A diffusive-coupling-induced stabilization of unstable equilibrium points is called amplitude death [3,4]. It has been proved that amplitude death never occurs in coupled identical oscillators [5–7]. However, Reddy *et al.* revealed that the diffusive time-delayed coupling causes amplitude death even in coupled identical oscillators [8,9]. Amplitude death by delayed coupling has attracted much attention in nonlinear science [10]. Various types of delayed couplings, which can induce amplitude death, have been reported, including distributed-delayed coupling [11–13], multiple-delayed coupling [14], time-varying delayed coupling [15–17], integrated delayed coupling [18], delayed multicomponent coupling [19], digital delayed coupling [20], mixed time-delayed coupling [21,22], and delayed mean-field coupling [23]. Furthermore, amplitude death induced by delay couplings is expected to be used for suppression of undesired oscillations in engineering systems, for instance coupled thermoacoustic systems [22] and dc micro grids [24].

Most previous studies on amplitude death assume that all coupling delays in coupled oscillators are identical in order to simplify the stability analysis. However, in real-world networks, such as neural networks [25], the coupling delays are often not identical due to physical constraints (e.g., different distances and propagation speeds of signals). For nonidentical coupling delays, the stability analysis of amplitude death is difficult, since the characteristic equation governing the stability cannot be simplified. Thus, for such a case, the stability of amplitude death must be estimated through numerical calculations [26]. To the best of our knowledge, there has been no analytical investigation of amplitude death induced by the nonidentical coupling delays.

The Cartesian product is one of the basic operations of graph theory [27]. This product allows us to make Cartesian product networks of two subnetworks [see Fig. 1(a)]. Various network topologies are made by the Cartesian product, for instance mesh graphs, cubic graphs, and hypercubic graphs. In Cartesian product networks, the Laplacian or adjacency matrices are easily diagonalized, and their eigenvalues are given by the sum of those of the two subnetworks. Based on

the above property, Atay and Bıyıkoğlu investigated complete synchronization in Cartesian product networks of diffusively coupled oscillators [28]. Asllani *et al.* studied Turing instability for a reaction-diffusion system defined on Cartesian product networks [29], and complete or partial synchronization in Cartesian product networks of delayed coupled oscillators has also been investigated [30,31].

As the first step in investigating amplitude death in networks with nonidentical coupling delays, the present study considers networks with two different coupling delays. In particular, we focus on Cartesian product networks of two subnetworks that have different coupling delays [see Fig. 1(a)]. We clarify the influence of these two coupling delays and topologies of the subnetworks on the stability of amplitude death. Recently, from an engineering viewpoint, design procedures for achieving desired dynamics in oscillator networks have attracted attention [32–35]. Hence, we propose two design procedures of coupling parameters (i.e., the coupling strength and coupling delays) for inducing amplitude death in the Cartesian product networks on the basis of the robust control theory. The design procedures do not require any information on the topologies of the subnetworks. The validity of the procedures is confirmed through numerical simulations. The present study is a substantially extended version of our conference paper [36].

The following notation is used throughout the present study. $\mathcal{G} = (\mathcal{V}, \mathcal{E})$ is a graph consisting of a set of nodes $\mathcal{V}$ and edges $\mathcal{E}$. Conversely, $\mathcal{V}(\mathcal{G})$ and $\mathcal{E}(\mathcal{G})$ represent the sets of nodes and edges, respectively, of the graph $\mathcal{G}$. $A_{\mathcal{G}}$ is the adjacency matrix of graph $\mathcal{G}$. If the ith and lth nodes are connected by an edge, then $\{A_{\mathcal{G}}\}_{il} = \{A_{\mathcal{G}}\}_{li} = 1$; otherwise, $\{A_{\mathcal{G}}\}_{il} = \{A_{\mathcal{G}}\}_{li} = 0$. I_N denotes the $N \times N$ unit matrix. The symbol $\otimes$ denotes the Kronecker product. The imaginary unit is defined as $j := \sqrt{-1}$.

II. CARTESIAN PRODUCT NETWORK OF DELAYED COUPLED OSCILLATORS

This section explains Cartesian product networks of delayed coupled oscillators. The Cartesian product is described mathematically on the basis of graph theory. The dynamics of
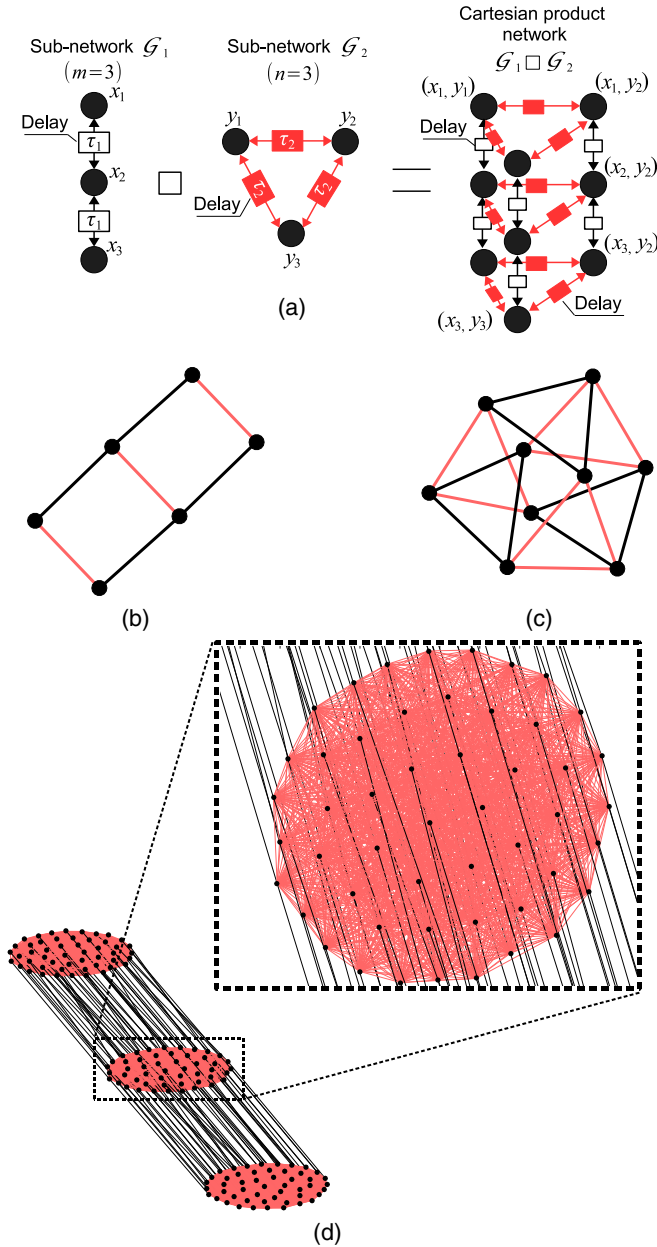
FIG. 1. Examples of Cartesian product networks $\mathcal{G}_1\square\mathcal{G}_2$ of delayed coupled oscillators. The networks consist of two subnetworks $\mathcal{G}_1$ and $\mathcal{G}_2$. Subnetworks $\mathcal{G}_1$ and $\mathcal{G}_2$, respectively, include the coupling delays τ_1 and τ_2, which are indicated by black and red (gray) frame squares for (a) and by black and red (gray) lines for (b)–(d). (a) $\mathcal{G}_1$: $m = 3$ path graph, $\mathcal{G}_2$: $n = 3$ ring graph. (b) $\mathcal{G}_1$: $m = 3$ path graph, $\mathcal{G}_2$: $n = 2$ path graph. (c) $\mathcal{G}_1$: $m = 3$ ring graph, $\mathcal{G}_2$: $n = 3$ ring graph. (d) $\mathcal{G}_1$: $m = 3$ path graph, $\mathcal{G}_2$: $n = 50$ complete graph.

the delayed coupled oscillators on Cartesian product networks is provided.

Let $\mathcal{V}_1 = \{x_1, \ldots, x_m\}$ and $\mathcal{V}_2 = \{y_1, \ldots, y_n\}$ be the node sets of graphs $\mathcal{G}_1 = (\mathcal{V}_1, \mathcal{E}_1)$ and $\mathcal{G}_2 = (\mathcal{V}_2, \mathcal{E}_2)$, respectively, where m and n are the numbers of nodes of $\mathcal{G}_1$ and $\mathcal{G}_2$. The Cartesian product network $\mathcal{G}_1\square\mathcal{G}_2$ of two subnetworks $\mathcal{G}_1$ and $\mathcal{G}_2$ is a graph for which the node set $\mathcal{V}(\mathcal{G}_1\square\mathcal{G}_2)$ is given by the Cartesian product $\mathcal{V}_1 \times \mathcal{V}_2$, that is, $\{(x_1, y_1), (x_1, y_2), \ldots, (x_m, y_n)\}$ [27]. An example of the

Cartesian product network is illustrated in Fig. 1(a), where the edges of the subnetworks $\mathcal{G}_1$ and $\mathcal{G}_2$ are indicated in black and red (gray), respectively. If two nodes (x_p, y_q) and $(x_{p'}, y_{q'})$, where $p, p' \in \{1, \ldots, m\}$ and $q, q' \in \{1, \ldots, n\}$, in $\mathcal{G}_1\square\mathcal{G}_2$ are adjacent, then we have $y_q = y_{q'}$ and $x_p x_{p'} \in \mathcal{E}(\mathcal{G}_1)$ or if $x_p = x_{p'}$ and $y_q y_{q'} \in \mathcal{E}(\mathcal{G}_2)$. For instance, as illustrated in Fig. 1(a), node (x_1, y_1) is adjacent to (x_1, y_2) but is not adjacent to (x_2, y_2). The adjacency matrix of the network $\mathcal{G}_1\square\mathcal{G}_2$ is given by

$$A_{\mathcal{G}_1\square\mathcal{G}_2} = A_{\mathcal{G}_1} \otimes I_n + I_m \otimes A_{\mathcal{G}_2}, \tag{1}$$

where $A_{\mathcal{G}_1} \in \mathbb{R}^{m \times m}$ and $A_{\mathcal{G}_2} \in \mathbb{R}^{n \times n}$. The first (second) term of the right-hand side of Eq. (1) represents $\mathcal{G}_1$ ($\mathcal{G}_2$) in $\mathcal{G}_1\square\mathcal{G}_2$ whose edges are illustrated by black (red) lines in Fig. 1(a).

The present study considers the Cartesian product network of delayed-coupled oscillators

$$\dot{Z}_i(t) = [\mu + j\omega - |Z_i(t)|^2]Z_i(t) + u_i^{(1)}(t) + u_i^{(2)}(t) \quad (i = 1, \ldots, mn), \tag{2}$$

where $Z_i(t) \in \mathbb{C}$ is the state variable of the ith oscillator, and $\mu > 0$ and $\omega > 0$ denote the instability and the natural frequency, respectively, of the equilibrium point $Z_i^* = 0$. Each oscillator receives the two signals $u_i^{(1)}(t)$ and $u_i^{(2)}(t)$ from subnetworks $\mathcal{G}_1$ and $\mathcal{G}_2$, which are given by

$$u_i^{(1)}(t) = k\left\{\frac{1}{d_i^{(1)}}\left(\sum_{l=1}^{mn} c_{i,l}^{(1)} Z_l(t - \tau_1)\right) - Z_i(t)\right\},$$

$$u_i^{(2)}(t) = k\left\{\frac{1}{d_i^{(2)}}\left(\sum_{l=1}^{mn} c_{i,l}^{(2)} Z_l(t - \tau_2)\right) - Z_i(t)\right\}, \tag{3}$$

where $k \in \mathbb{R}$ denotes the coupling strength, and $\tau_1 \geqslant 0$ and $\tau_2 \geqslant 0$ are the coupling delays in the subnetworks $\mathcal{G}_1$ and $\mathcal{G}_2$, respectively [see Fig. 1(a)]. $c_{i,l}^{(1)}$ and $c_{i,l}^{(2)}$ represent the (i, l) elements of the adjacency matrices of $A_{\mathcal{G}_1} \otimes I_n$ and $I_m \otimes A_{\mathcal{G}_2}$ in Eq. (1), respectively: if the ith and the lth oscillators are coupled in the subnetwork $\mathcal{G}_1$ ($\mathcal{G}_2$), then $c_{i,l}^{(1)} = c_{l,i}^{(1)} = 1$ ($c_{i,l}^{(2)} = c_{l,i}^{(2)} = 1$), otherwise $c_{i,l}^{(1)} = c_{l,i}^{(1)} = 0$ ($c_{i,l}^{(2)} = c_{l,i}^{(2)} = 0$). Here, $d_i^{(1),(2)} := \sum_{l=1}^{mn} c_{i,l}^{(1),(2)}$ are the degrees of the ith oscillator in subnetworks $\mathcal{G}_{1,2}$. Coupled oscillators (2) and (3) have a homogeneous steady state,

$$[Z_1^*, \ldots, Z_{mn}^*]^T = [0, \ldots, 0]^T. \tag{4}$$

If steady state (4) is stable, amplitude death can occur.

Our motivation is to clarify the influence of the two coupling delays and the topologies of subnetworks on the stability of the steady state (4) (i.e., the local stability of amplitude death).

III. STABILITY ANALYSIS

This section investigates the local stability of steady state (4). Linearizing coupled oscillators (2) and (3) at state (4), we

obtain the linearized equation

$$\dot{z}_i(t) = (\mu + j\omega - 2k)z_i(t)$$
$$+ \frac{k}{d_i^{(1)}} \sum_{l=1}^{mn} c_{i,l}^{(1)} z_l(t - \tau_1) + \frac{k}{d_i^{(2)}} \sum_{l=1}^{mn} c_{i,l}^{(2)} z_l(t - \tau_2), \quad (5)$$

where $z_i(t) := Z_i(t) - Z_i^*$ is a perturbation from the equilibrium point. Equation (5) can be rewritten as

$$\dot{X}(t) = (\mu + j\omega - 2k)X(t) + k(E_1 \otimes I_n)X(t - \tau_1)$$
$$+ k(I_m \otimes E_2)X(t - \tau_2), \quad (6)$$

where $X(t) := [z_1(t), \ldots, z_{mn}(t)]^T$. Matrices $E_1 := D_{\mathcal{G}_1}^{-1} A_{\mathcal{G}_1}$ and $E_2 := D_{\mathcal{G}_2}^{-1} A_{\mathcal{G}_2}$ are the normalized adjacency matrices of the subnetworks, where $D_{\mathcal{G}_1} \in \mathbb{R}^{m \times m}$ and $D_{\mathcal{G}_2} \in \mathbb{R}^{n \times n}$ are the degree matrices of $\mathcal{G}_1$ and $\mathcal{G}_2$, respectively.

The stability of linear system (6) is governed by the characteristic function,

$$G(s) = \det[(s - \mu - j\omega + 2k)I_{mn}$$
$$- k\{(E_1 \otimes I_n)e^{-s\tau_1} + (I_m \otimes E_2)e^{-s\tau_2}\}]. \quad (7)$$

Here, matrices E_1 and E_2 are similar to real symmetric matrices [37]. Thus, by transformation matrices T_1 and T_2, matrices E_1 and E_2 are diagonalized as follows:

$$T_1^{-1} E_1 T_1 = \text{diag}(\rho_1, \ldots, \rho_m),$$
$$T_2^{-1} E_2 T_2 = \text{diag}(\sigma_1, \ldots, \sigma_n),$$

where $\rho_1, \ldots, \rho_m \in \mathbb{R}$ and $\sigma_1, \ldots, \sigma_n \in \mathbb{R}$ are the eigenvalues of E_1 and E_2, respectively. This diagonalization allows us to rewrite Eq. (7) as

$$G(s) = \det\left[\left(T_1^{-1} \otimes T_2^{-1}\right)[(s - \mu - j\omega + 2k)I_{mn}\right.$$
$$- k\{(E_1 \otimes I_n)e^{-s\tau_1} + (I_m \otimes E_2)e^{-s\tau_2}\}](T_1 \otimes T_2)\Big]$$
$$= \det[(s - \mu - j\omega + 2k)I_{mn}$$
$$- k\{[\text{diag}(\rho_1, \ldots, \rho_m) \otimes I_n]e^{-s\tau_1}$$
$$+ [I_m \otimes \text{diag}(\sigma_1, \ldots, \sigma_n)]e^{-s\tau_2}\}].$$

Thus, Eq. (7) can be separated into mn modes,

$$G(s) = \prod_{p=1}^{m} \left\{ \prod_{q=1}^{n} g(s, \rho_p, \sigma_q) \right\},$$

where

$$g(s, \rho, \sigma) := s - \mu - j\omega + 2k - k(\rho e^{-s\tau_1} + \sigma e^{-s\tau_2}). \quad (8)$$

We see that steady state (4) is stable if and only if all the mn modes of $g(s, \rho, \sigma)$ are stable. In the following, we investigate the stability of the characteristic function (8).

Note that the stability is changed when at least one root of $g(s, \rho, \sigma) = 0$ crosses the imaginary axis in the complex plane. The root on the imaginary axis is a pure imaginary number. Substituting $s = j\lambda$ ($\lambda \in \mathbb{R}$) into $g(s, \rho, \sigma) = 0$ yields its real and imaginary parts,

$$-\mu + 2k - k\rho \cos(\lambda\tau_1) - k\sigma \cos(\lambda\tau_2) = 0,$$
$$\lambda - \omega + k\rho \sin(\lambda\tau_1) + k\sigma \sin(\lambda\tau_2) = 0. \quad (9)$$

From Eq. (9), the marginal stability curve and stability region are derived by the following procedure. First, by solving Eq. (9) in terms of $\tau_{1,2}$ using a numerical approach such as the Newton-Raphson method, we can derive the marginal stability curves on the coupling delays space (τ_1, τ_2) [14]. Second, by checking the direction of the root crossing the imaginary axis, we can estimate the stability region. The direction is decided by the sign of the following equation:

$$\text{Re}\left[\frac{ds}{d\tau_2}\right]_{s=j\lambda} = \text{Re}\left[-\frac{j\lambda k\sigma e^{-j\lambda\tau_2}}{1 + k\left(\rho\tau_1 e^{-j\lambda\tau_1} + \sigma\tau_2 e^{-j\lambda\tau_2}\right)}\right]. \quad (10)$$

A positive (negative) sign in Eq. (10) indicates that the root crosses the imaginary axis from left to right (right to left) with increasing τ_2.

IV. STABILITY REGION

To examine the influence of the two coupling delays (i.e., τ_1, τ_2) and the topologies of subnetworks (i.e., ρ_p, σ_q) on the stability of amplitude death, this section derives the stability curve and region based on the procedure explained in the previous section. The parameters of the oscillators are fixed at

$$\mu = 0.5, \quad \omega = 2\pi. \quad (11)$$

The coupling strength is set to $k = 3\mu = 1.5$. Figures 2(a)–2(d) show the stability curves and regions in space (τ_1, τ_2) for the four different Cartesian product networks illustrated in Figs. 1(a)–1(d), respectively: (a) $\mathcal{G}_1$: $m = 3$ path graph ($\rho_1 = 1, \rho_2 = 0, \rho_3 = -1$), $\mathcal{G}_2$: $n = 3$ ring graph ($\sigma_1 = 1, \sigma_{2,3} = -0.5$); (b) $\mathcal{G}_1$: $m = 3$ path graph, $\mathcal{G}_2$: $n = 2$ path graph ($\sigma_1 = 1, \sigma_2 = -1$); (c) $\mathcal{G}_1$: $m = 3$ ring graph, $\mathcal{G}_2$: $n = 3$ ring graph; and (d) $\mathcal{G}_1$: $m = 3$ path graph, $\mathcal{G}_2$: $n = 50$ complete graph ($\sigma_1 = 1, \sigma_{2,\ldots,50} = -1/49$). The thin and bold curves represent the stability boundaries. If a parameter set (τ_1, τ_2) crosses the bold (thin) curve with an increase in τ_2, at least one root of $g(s, \rho, \sigma) = 0$ crosses the imaginary axis from right to left (left to right). The gray areas denote the stability region of amplitude death, where all roots of $g(s, \rho, \sigma) = 0$ remain in the open left-half plane.

We can see that the stability region depends heavily on the network topology of the subnetworks. For instance, Fig. 2(b) has a narrow region, whereas Fig. 2(c) has a wide region. Furthermore, the long coupling delays of the two subnetworks cannot induce amplitude death if the delays are the same (i.e., $\tau_1 = \tau_2$) [8]. For example, the parameter set $(\tau_1, \tau_2) = (1.25, 1.25)$, both of whose elements are somewhat longer than the period of the oscillator $T = 2\pi/\omega = 1.0$, is out of the stability region in all Figs. 2(a)–2(d) (see the black cross symbols in Fig. 2). In contrast, for different coupling delays (i.e., $\tau_1 \neq \tau_2$), we can induce amplitude death even for long coupling delays (see the white dotted lines in Fig. 2). Note that these white dotted lines are commonly observed in Fig. 2 regardless of the different topologies of the subnetworks.

In the next section, we will theoretically prove that these white dotted lines exist independently of the topologies of the subnetworks. Furthermore, based on the above fact, two design procedures of the coupling parameters (i.e., the
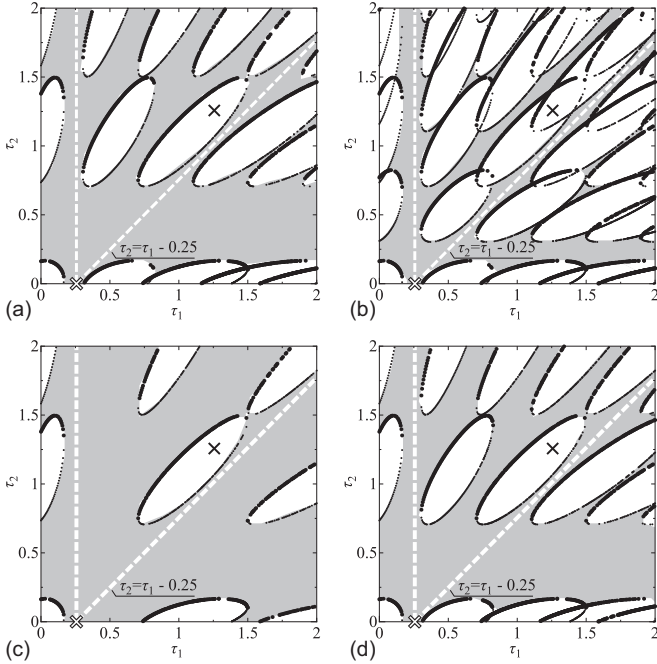
FIG. 2. Stability curves and regions (gray areas) on the coupling delays space (τ_1,τ_2) for the four Cartesian product networks $\mathcal{G}_1 \square \mathcal{G}_2$ illustrated in Fig. 1: (a) G_1: $m = 3$ path graph, G_2: $n = 3$ ring graph; (b) G_1: $m = 3$ path graph, G_2: $n = 2$ path graph; (c) G_1: $m = 3$ ring graph, G_2: $n = 3$ ring graph; and (d) G_1: $m = 3$ path graph, G_2: $n = 50$ complete graph. The parameters of the oscillators are fixed at $(\mu,\omega) = (0.5,2\pi)$. The coupling strength is set to $k = 3\mu = 1.5$. The black cross symbol at $(\tau_1,\tau_2) = (1.25,1.25)$ represents the point where the two coupling delays in two subnetworks are somewhat longer than the period of the oscillator $T = 2\pi/\omega = 1.0$. The vertical and diagonal white dotted lines through the white cross symbol [i.e., $(\tau_1,\tau_2) = (0.25,0)$] are $\tau_1 = 0.25$ and $\tau_2 = \tau_1 - 0.25$, respectively.

coupling delays τ_1,τ_2 and the coupling strength k) for inducing amplitude death will be provided.

V. DESIGN PROCEDURE

The previous section shows that the stability region depends heavily on the network topology of the subnetworks. Thus, in order to induce amplitude death, we have to know the topology in advance. However, it would be difficult to obtain the network topology in detail for a large-scale network. This section proposes topology-free design procedures of coupling parameters (k,τ_1,τ_2) for inducing amplitude death.

Now, we consider the coupling parameters (k,τ_1,τ_2), which induce steady state (4) to be stable for an arbitrary topology of the subnetworks. Here, ρ and σ in Eq. (8) are the parameters depending on the topology of the subnetworks. It is known that these two values always satisfy $\rho \in [-1,1]$ and $\sigma \in [-1,1]$ for any network topologies[1] [38]. Hence, steady state (4) is stable independent of the topologies of the subnetworks if

---

[1]For example, the eigenvalues set (ρ_p,σ_q) for the network illustrated in Fig. 1(d) is plotted as the red (gray) cross symbols in space (ρ,σ) in Fig. 3.
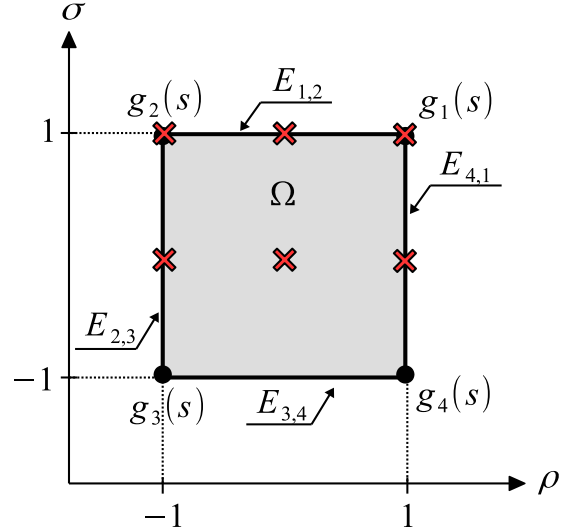

FIG. 3. Convex family Ω in the (σ,ρ) space (gray region). Edges $E_{\gamma,\eta}$ with vertices $g_\gamma(s)$ and $g_\eta(s)$ envelopes Ω. Red (gray) cross symbols indicate eigenvalues (σ_p,ρ_q) for the network illustrated in Fig. 1(d).

characteristic function (8) is stable for any $\rho \in [-1,1]$ and $\sigma \in [-1,1]$. However, it is difficult to check the stability of Eq. (8) for all ρ and σ.

Robust control theory helps us to address this difficulty in stability analysis. Since ρ and σ have upper and lower limits, Eq. (8) can be expressed as the elements of the convex family (see Fig. 3):

$$\Omega := \{g(s,\rho,\sigma) \mid \rho \in [-1,1], \sigma \in [-1,1]\}$$
$$= \text{conv}\{g_1(s),g_2(s),g_3(s),g_4(s)\}, \quad (12)$$

where the four vertices of Ω are given by

$$g_1(s) := g(s,1,1), \quad g_2(s) := g(s,-1,1),$$
$$g_3(s) := g(s,-1,-1), \quad g_4(s) := g(s,1,-1).$$

The edge theorem [39,40] in robust control theory guarantees that Ω is stable if and only if all the edges,

$$E_{\gamma,\eta} := (1-\alpha)g_\gamma(s) + \alpha g_\eta(s), \quad \alpha \in [0,1], \quad (13)$$

with $(\gamma,\eta) \in \{(1,2), (2,3), (3,4), (4,1)\}$ enveloping Ω, are stable (see Fig. 3). In other words, in order to guarantee the stability of steady state (4) for any topologies of the subnetworks, we only have to check the stability of these four edges.

The present study proposes two design procedures based on the edge theorem. In preparation for these procedures, we present the following topology-free lemma:

Lemma 1. Assume that the parameters of the oscillators satisfy

$$\omega \geqslant 2\pi\mu. \quad (14)$$

Steady state (4) is stable for any number of oscillators m,n and any topologies of the subnetworks $\boldsymbol{E}_1$ and $\boldsymbol{E}_2$ if the coupling

strength and coupling delays are set to

$$k = 3\mu, \tag{15}$$

$$\tau_1 = \frac{\pi}{2\omega}, \tag{16}$$

$$\tau_2 = 0. \tag{17}$$

Proof. We will show that all of the edges (13) are stable if the coupling parameters are set to Eqs. (15), (16), and (17). See Appendix A for additional details.

Note that Lemma 1 holds if τ_1 is swapped for τ_2, since this lemma does not depend on the topologies of the subnetworks. Note that $k = 3\mu = 1.5$ is fixed in accordance with Eq. (15) in Fig. 2. We can see that the point $(\tau_1, \tau_2) = (0.25, 0)$ for Eqs. (16) and (17) (see the white cross symbols) remains in the stability regions despite the different subnetworks.

On the basis of Lemma 1, we propose two design procedures. The first procedure is useful when one of the coupling delays in the subnetworks must be long.

Theorem 1. Assume that the parameters of the oscillators satisfy inequality (14). Steady state (4) is stable for arbitrary coupling delay $\tau_2 \geqslant 0$, any number of oscillators m, n, and any topologies of subnetworks $\boldsymbol{E}_1$ and $\boldsymbol{E}_2$ if the coupling strength k and coupling delay τ_1 are set to Eqs. (15) and (16), respectively.

Proof. Lemma 1 guarantees the stability of $g(s, \sigma, \rho)$ with $\tau_2 = 0$ for any $\sigma \in [-1, 1]$ and $\rho \in [-1, 1]$. Here, we prove that the stability of $g(s, \sigma, \rho)$ is maintained even for any $\tau_2 \geqslant 0$. This proof will show that $g(i\lambda, \rho, \sigma) = 0$ [i.e., Eq. (9)] has no root for any $\tau_2 \geqslant 0$ if the coupling parameters (k, τ_1) are set to Eqs. (15) and (16). See Appendix B for further details.

The vertical dotted lines in Fig. 2 indicate $\tau_1 = 0.25$ [i.e., Eq. (16)]. It can be seen that, in all of Figs. 2(a)–2(d), these lines exist within the stability region. Thus, we can choose arbitrarily long τ_2.

Theorem 1 shows that one of the coupling delays can be chosen arbitrarily, but another has to be fixed at Eq. (16). Hence, we cannot choose both of the coupling delays to be long. If both coupling delays must be long, then the following theorem is useful for their design:

Theorem 2. Assume that the parameters of oscillators satisfy inequality (14). Steady state (4) is stable for any number of oscillators m, n and any topologies of subnetworks $\boldsymbol{E}_1$ and $\boldsymbol{E}_2$ if the coupling strength k is set to Eq. (15) and the two coupling delays (τ_1, τ_2) satisfy

$$\tau_2 = \tau_1 - \frac{\pi}{2\omega}. \tag{18}$$

Proof. Note that Lemma 1 guarantees the stability of $g(s, \sigma, \rho)$ for any $\sigma \in [-1, 1]$ and $\rho \in [-1, 1]$ when the coupling delays are set to Eq. (18) with $\tau_1 = \pi/(2\omega)$. Here, we show that the stability of $g(s, \rho, \sigma)$ is maintained as long as Eq. (18) is satisfied for $\tau_1 \geqslant \pi/(2\omega)$. In other words, we prove that there is no root of $g(i\lambda, \rho, \sigma) = 0$ [i.e., Eq. (9)] when Eq. (18) is satisfied. See Appendix C for further details.

The diagonal dotted lines in Fig. 2 indicate Eq. (18). We can see that these lines are commonly observed in Fig. 2.

Note that both Theorems 1 and 2 hold if τ_1 is swapped for τ_2 since these theorems are independent of the topologies of the subnetworks. It must be emphasized that we can design the

coupling parameters by Theorems 1 and 2 even if we do not know the topologies of the subnetworks.

The previous design procedures for inducing amplitude death (e.g., [14,17]) have a severe constraint on the coupling delays, that is, the procedures can be applied to networks only with identical coupling delays. Thus, the range of application of the previous procedures is limited. On the other hand, the design procedures in the present study would relax this constraint, since we can design the two different coupling delays for inducing amplitude death. It should be noted, however, that our procedures can be used only for the Cartesian product networks.

Amplitude death is sometimes undesirable and should be avoided in real-world applications. Thus, some researchers have investigated the control method for avoiding amplitude death or the condition of revoking amplitude death (i.e., from amplitude death to oscillatory behaviors) [41,42]. In the present study, the edge theorem is used to guarantee robust stability against topology uncertainty. Thus, if one can extend the edge theorem to guarantee the instability, then it may be possible to analyze revoking amplitude death.

VI. NUMERICAL EXAMPLE

Let us design the coupling parameters in accordance with Theorems 1 and 2. The parameters of the oscillators are fixed at Eq. (11).

First, we use Theorem 1. The parameters (11) satisfy inequality (14). The coupling strength is set to $k = 1.5$ [i.e., Eq. (15)], and one of the coupling delays is set to $\tau_1 = 0.25$ [i.e., Eq. (16)]. Then, Theorem 1 guarantees the stability for arbitrary τ_2. Here, we choose $\tau_2 = 10$. Figure 4(a) shows the time-series data with the designed parameters (k, τ_1, τ_2) for the network illustrated in Fig. 1(d). The top graph is the state variable of the first oscillator $\mathrm{Re}[Z_1(t)]$, and the bottom graph is the sum of the perturbations from the equilibrium point, $\sum_{i=1}^{150} |Z_i(t) - Z_i^*|$. All of the oscillators are independent of each other until $t = 30$. At $t = 30$, they are coupled with the designed parameters $(k, \tau_1, \tau_2) = (1.5, 0.25, 10)$. After coupling, all of the oscillators converge to the equilibrium point.

Second, we confirm Theorem 2. As in the case of Theorem 1, assumption (14) holds, then the coupling strength is set to $k = 1.5$. Theorem 2 guarantees the stability of the steady state if the two coupling delays satisfy Eq. (18). Here, we choose long coupling delays $\tau_1 = 10.25$ and $\tau_2 = 10$. Figure 4(b) shows the time-series data for the network illustrated in Fig. 1(d). After coupling with the designed parameters (k, τ_1, τ_2), we can see that oscillation of all the oscillators is suppressed.

VII. DISCUSSION

Multiple-delay coupling was proposed in a previous study [14]. For this coupling, two oscillators in networks are coupled with two different transmission paths. Thus, as in the present study, multiple-delay coupling has two different delays. This section compares the results of the previous study [14] to those of the present study.

The previous study reported that multiple-delay coupling with long identical delays cannot induce amplitude death [14].
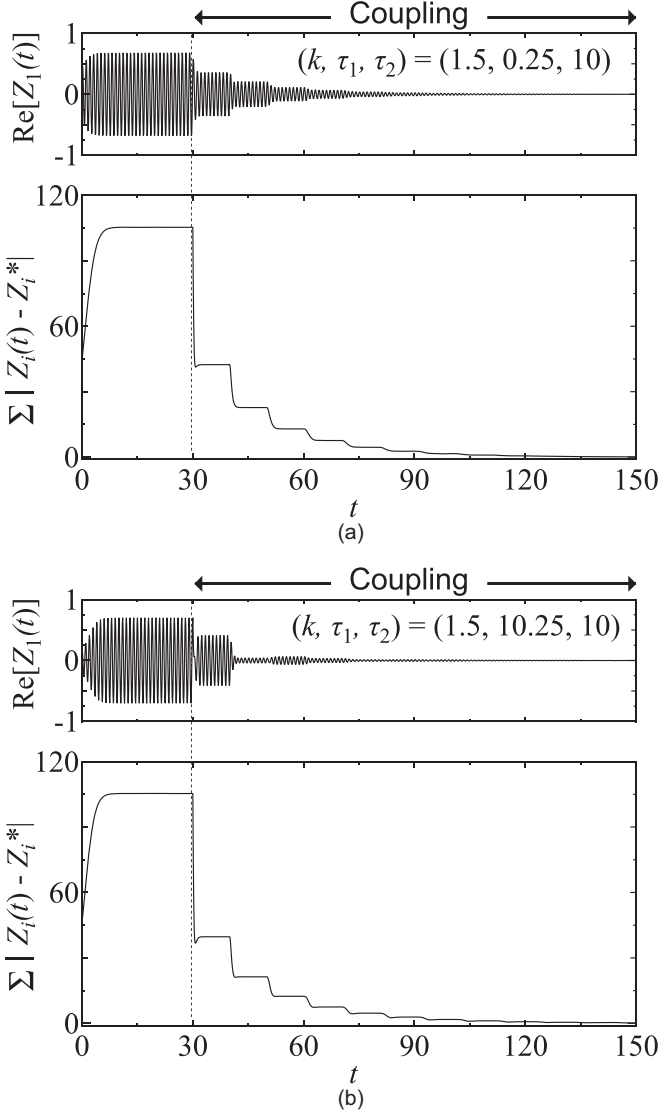
FIG. 4. Time-series data for the network illustrated in Fig. 1(d). The top and bottom graphs show the state variable of first oscillator and the sum of the perturbation from the equilibrium point, respectively. The parameters of the oscillators are fixed at $(\mu,\omega) = (0.5, 2\pi)$. All of the oscillators are independent until $t = 30$ and are coupled with the designed parameters at $t = 30$. (a) $(k,\tau_1,\tau_2) = (1.5, 0.25, 10)$ and (b) $(k,\tau_1,\tau_2) = (1.5, 10.25, 10)$.

In contrast, if there is a suitable difference, then amplitude death can occur for two long coupling delays. It has been proven that this is independent of the network topology. From an engineering point of view, the multiple-delay connection has a high cost, since this coupling requires two transmission paths between oscillators.

As in the previous study, the present study shows that long identical coupling delays of the two subnetworks cannot induce amplitude death (see Fig. 2). However, if there is a suitable difference between the delays, then we can induce amplitude death for long coupling delays (see Theorem 1). Compared to multiple-delay coupling, we require only one transmission path between oscillators, but the topology is limited to the Cartesian product networks.

VIII. CONCLUSION

The present study investigated amplitude death in the Cartesian product networks of two subnetworks. We showed that long coupling delays can induce amplitude death if there is a suitable difference in the coupling delays of the two subnetworks. Furthermore, we proposed two design procedures of the coupling parameters for inducing amplitude death. Our procedures do not require any information on the topology of the subnetworks. Numerical simulations verified the validity of our procedures.

ACKNOWLEDGMENTS

APPENDIX A: PROOF OF LEMMA 1

We first focus on the stability of edge $E_{1,2}$. This edge is stable if and only if both of the following conditions are satisfied [43]:

Condition (i): $g_1(s)$ and $g_2(s)$ are stable.

Condition (ii): $\phi(\lambda) := \arg[g_1(j\lambda)] - \arg[g_2(j\lambda)] \neq \pm\pi$, $\forall\,\lambda \in \mathbb{R}$.

Condition (i) requires that the nodes of edge $E_{1,2}$ [i.e., $\alpha = 0$ and 1 in Eq. (13)] be stable. Condition (ii) requires that the stability of $g(s,\rho,\sigma)$ be maintained even if α varies within $\alpha \in [0,1]$.

First, let us consider condition (i). We investigate the stability of node $g_1(s)$ by the direct method [44]. Here, (k,τ_2) are fixed as Eqs. (15) and (17). In the following, τ_1 is treated as a variable parameter. Then, $g_1(s) = 0$ can be written as

$$P(s) + Qe^{-s\tau_1} = 0, \qquad (A1)$$

where $P(s) := s + 2\mu - j\omega$ and $Q := -3\mu$. The stability of $g_1(s)$ is changed when at least one root of $g_1(s) = 0$ crosses the imaginary axis. Substituting $s = j\lambda$ into $g_1(s) = 0$ yields

$$-Q/P(j\lambda) = e^{j\lambda\tau_1}. \qquad (A2)$$

Equation (A2) can be divided into two parts, amplitude and phase:

$$F_p(\lambda) := P(j\lambda)\overline{P(j\lambda)} - Q^2 = 0, \qquad (A3)$$

$$\lambda\tau_1 = \arg\left(-\frac{Q}{P(j\lambda)}\right) + 2\pi r, \quad r = 0, \pm 1, \pm 2, \ldots, \quad (A4)$$

where $\bar{x}$ is the complex conjugate of x. By solving Eq. (A3) in terms of λ, we obtain $\lambda_\pm := \omega \pm \mu\sqrt{5}$. This means that a root of Eq. (A1) crosses the point $\lambda = i\lambda_\pm$ on the imaginary axis as τ_1 varies. The direction in which the root crosses the imaginary axis can be decided by

$$\text{sgn}\left(\text{Re}\left.\frac{ds}{d\tau_1}\right|_{s=i\lambda}\right) = \text{sgn}(\lambda)\text{sgn}\left(\frac{dF_p(\lambda)}{d\lambda}\right)$$
$$= \text{sgn}[\lambda(\lambda - \omega)]. \qquad (A5)$$

Here, Eq. (A5) is negative for $\lambda = \lambda_-$ and positive for $\lambda = \lambda_+$. This means that, with increasing τ_1, the root crosses the point

$\lambda = i\lambda_- \ (\lambda = i\lambda_+)$ on the imaginary axis from right to left (left to right). The coupling delay τ_1 at that point is calculated from Eq. (A4),

$$\tau_\pm(r) := \frac{1}{\lambda_\pm}\left\{\arg\left(-\frac{Q}{P(j\lambda_\pm)}\right) + 2\pi r\right\}. \quad \text{(A6)}$$

For $\tau_1 = 0$, $g_1(s) = 0$ has an unstable root $s = \mu + i\omega$. With increasing τ_1, when τ_1 exceeds $\tau_1 = \tau_-(0)$, then the root crosses the imaginary axis from right to left, and $g_1(s)$ becomes stable. Further increasing τ_1, when τ_1 exceeds $\tau_1 = \tau_+(0)$, then the root crosses the imaginary axis from left to right, and $g_1(s)$ becomes unstable. The above discussion can be summarized as follows: $g_1(s)$ is stable if the coupling delay τ_1 holds at $\tau_-(0) < \tau_1 < \tau_+(0)$. Moreover, inequality $\tau_-(0) < \pi/(2\omega) < \tau_+(0)$ is satisfied. Therefore, node $g_1(s)$ is stable if the coupling delay τ_1 is set to Eq. (16). By the same procedure, we can guarantee the stability of the node $g_2(s)$. Thus, condition (i) is satisfied.

Next, we consider condition (ii). We show that the absolute value of angle $|\phi(\lambda)|$ between the two vectors $g_1(i\lambda)$ and $g_2(i\lambda)$ on the complex plane is less than π. The inner product of $g_1(i\lambda)$ and $g_2(i\lambda)$ is given by

$$(\lambda - \omega)^2 - 5\mu^2. \quad \text{(A7)}$$

The inner product (A7) is negative if $|\phi(\lambda)|$ is greater than $\pi/2$. The range of λ for Eq. (A7) being negative is $\omega - \sqrt{5}\mu < \lambda < \omega + \sqrt{5}\mu$. We can easily check that, in this range of λ, the sign of both $\text{Re}[g_1(j\lambda)]$ and $\text{Re}[g_2(j\lambda)]$ is always positive. This indicates that angle $\phi(\lambda)$ always satisfies $|\phi(\lambda)| < \pi$, $\forall \lambda \in \mathbb{R}$. Hence, condition (ii) holds.

Conditions (i) and (ii) prove that edge $E_{1,2}$ is stable. Using the same procedure, we can prove that all edges (13) are stable. Therefore, the edge theorem guarantees that, under the assumption (14), the family Ω is stable if the coupling parameters are set to Eqs. (15), (16), and (17). ∎

APPENDIX B: PROOF OF THEOREM 1

We fixed the coupling delay τ_1 and the coupling strength k at Eqs. (16) and (15), respectively. By $\sin^2(\lambda\tau_2) + \cos^2(\lambda\tau_2) = 1$, we can eliminate τ_2 from Eq. (9),

$$F(\lambda,\rho) := (\lambda - \omega)^2 + \{25 + 9(\rho^2 - \sigma^2)\}\mu^2$$
$$- 6\mu\rho\left\{5\mu\cos\left(\lambda\frac{\pi}{2\omega}\right) + (\omega - \lambda)\sin\left(\lambda\frac{\pi}{2\omega}\right)\right\}$$
$$= 0. \quad \text{(B1)}$$

If there is no root of $F(\lambda,\rho) = 0$, then there is no λ satisfying Eq. (9). We prove that $F(\lambda,\rho) > 0$, $\forall \lambda \in \mathbb{R}$. Note that we only have to check either $\rho \geqslant 0$ or $\rho \leqslant 0$, since $F(\omega - \lambda, \rho) = F(\omega + \lambda, -\rho)$ holds: that is, the two functions $F(\lambda,\rho)$ and $F(\lambda, -\rho)$ of λ are symmetric with respect to the line $\lambda = \omega$. In the following, we consider $\rho \geqslant 0$ (i.e., $\rho \in [0,1]$). We divide $\lambda \in \mathbb{R}$ into the following four ranges: (i) $\lambda \leqslant 0$, (ii) $0 \leqslant \lambda \leqslant \omega$, (iii) $\omega \leqslant \lambda \leqslant 2\omega$, and (iv) $2\omega \leqslant \lambda$.

For (i) $\lambda \leqslant 0$, we define the following function:

$$F_1(\lambda) := (\lambda - \omega)^2 + 16\mu^2 - 6\mu\sqrt{25\mu^2 + (\lambda - \omega)^2}. \quad \text{(B2)}$$

Obviously, $F(\lambda,\rho) \geqslant F_1(\lambda)$ holds in range (i). $F_1(\lambda)$ is a monotonically decreasing function with respect to λ within
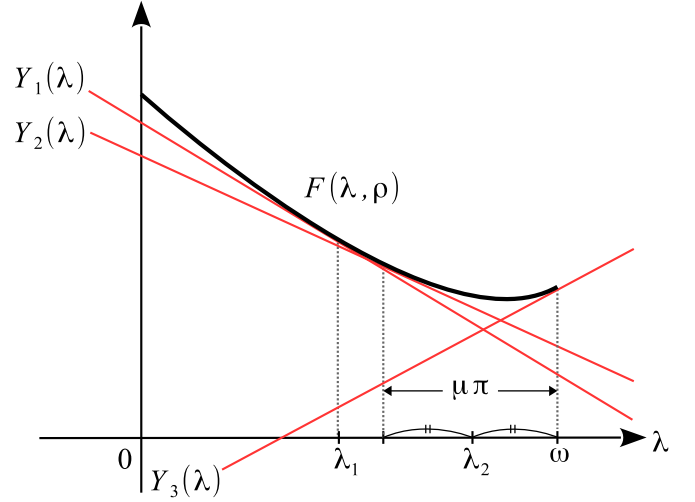

FIG. 5. A sketch of the function $F(\lambda,\rho)$ for $0 \leqslant \lambda \leqslant \omega$. Tangent lines at $\lambda = \lambda_1$, $\omega - \mu\pi$, and ω are, respectively, denoted by $Y_1(\lambda)$, $Y_2(\lambda)$, and $Y_3(\lambda)$.

range (i), and its minimum value is given by

$$\underline{F_1}(\omega) := F_1(0) = \omega^2 + 16\mu^2 - 6\mu\sqrt{25\mu^2 + \omega^2}. \quad \text{(B3)}$$

Furthermore, $\underline{F_1}(\omega)$ is a monotonically increasing function with respect to ω. Thus, its minimum value is given by

$$\min_{\omega \geqslant 2\pi\mu} \underline{F_1}(\omega) = \underline{F_1}(2\pi\mu) > 0. \quad \text{(B4)}$$

Therefore, $F(\lambda,\rho) \geqslant F_1(\lambda) \geqslant \underline{F_1}(\omega) \geqslant \underline{F_1}(2\pi\mu) > 0$ holds.

For (ii) $0 \leqslant \lambda \leqslant \omega$, since the second derivative of $F(\lambda,\rho)$ in terms of λ satisfies $F''(\lambda,\rho) > 0$, the function $F(\lambda,\rho)$ is convex in range (ii) (see Fig. 5). Let us consider the tangent lines to the function $F(\lambda,\rho)$ at $\lambda = \lambda_1$, $\omega - \mu\pi$, and ω, respectively,

$$Y_1(\lambda) := F'(\lambda_1,\rho)(\lambda - \lambda_1) + F(\lambda_1,\rho),$$
$$Y_2(\lambda) := F'(\omega - \mu\pi,\rho)(\lambda - \omega + \mu\pi) + F(\omega - \mu\pi,\rho),$$
$$Y_3(\lambda) := F'(\omega,\rho)(\lambda - \omega) + F(\omega,\rho),$$

where $\lambda_1 := 3\omega/4 - \mu\pi/2$. We can easily check that these tangent lines satisfy the following conditions: (a) $Y_1(\lambda)$ has a negative slope; (b) $Y_2(\lambda)$ is positive at $\lambda = \lambda_1$; (c) $Y_2(\lambda)$ is positive at $\lambda = \lambda_2 := \omega - \mu\pi/2$; (d) $Y_3(\lambda)$ has a positive slope; and (e) $Y_3(\lambda)$ is positive at $\lambda = \lambda_2$. It is known that the graph of a convex function lies above all of its tangent lines, that is, $F(\lambda,\rho) \geqslant Y_{1,2,3}(\lambda)$ is satisfied in range (ii). Thus, considering the conditions (a)–(e), we have the following facts: $F(\lambda,\rho) > 0$ for $0 \leqslant \lambda \leqslant \lambda_1$ from (a) and (b), $F(\lambda,\rho) > 0$ for $\lambda_1 \leqslant \lambda \leqslant \lambda_2$ from (b) and (c), and $F(\lambda,\rho) > 0$ for $\lambda_2 \leqslant \lambda \leqslant \omega$ from (d) and (e). As a result, $F(\lambda,\rho) > 0$ holds for $0 \leqslant \lambda \leqslant \omega$.

For (iii) $\omega \leqslant \lambda \leqslant 2\omega$, we consider

$$F_3(\lambda) := (\lambda - \omega)^2 + (16 + 9\rho^2)\mu^2 + \frac{30\mu^2\rho(\lambda - \omega)}{\omega}. \quad \text{(B5)}$$

Since $\cos[\lambda\pi/(2\omega)] \leqslant -(\lambda - \omega)/\omega$ and $(\omega - \lambda)\sin[\lambda\pi/(2\omega)] \leqslant 0$ are satisfied in range (iii), we notice that $F(\lambda,\rho) \geqslant F_3(\lambda)$ holds. We can easily check that all the

terms on the right-hand side of Eq. (B5) are greater than or equal to zero. Therefore, we have $F(\lambda,\rho) \geqslant F_3(\lambda) > 0$.

For (iv) $2\omega \leqslant \lambda$, let us consider the function

$$F_4(\lambda) := (\lambda - \omega)^2 + (16 + 9\rho^2)\mu^2$$
$$- 6\mu\rho\left\{5\mu\cos\left(\lambda\frac{\pi}{2\omega}\right) + \lambda - \omega\right\}. \quad (B6)$$

Obviously, $F(\lambda,\rho) \geqslant F_4(\lambda)$ holds in range (iv). Since $F_4''(\lambda) > 0$ holds, $F_4'(\lambda)$ is a monotonically increasing function. Furthermore, as the minimum value of $F_4'(\lambda)$ [i.e., $F_4'(2\omega)$] is positive, $F_4(\lambda)$ is a monotonically increasing function. As a result, the minimum value of $F_4(\lambda)$ is given by

$$F_4(2\omega) = (\omega - 3\mu\rho)^2 + 16\mu^2 + 30\mu^2\rho > 0.$$

Therefore, $F(\lambda,\rho) \geqslant F_4(\lambda) > 0$ holds.

From (i) to (iv), $F(\lambda,\rho) > 0$ holds for $\forall \lambda \in \mathbb{R}$. Thus, there is no λ satisfying Eq. (9) for any $\sigma \in [-1,1]$ and $\rho \in [-1,1]$ when the coupling parameters (k,τ_1) are set to Eqs. (15) and (16). In other words, the stability of the steady state is maintained independent of τ_2. Moreover, Lemma 1 guarantees that $g(s,\rho,\sigma)$ is stable for $\tau_2 = 0$. Therefore, $g(s,\rho,\sigma)$ with Eqs. (15) and (16) is stable for arbitrarily long coupling delay τ_2. ∎

APPENDIX C: PROOF OF THEOREM 2

Substituting Eqs. (15) and (18) into Eq. (9) yields

$$\cos(\lambda\tau_1)\left\{\rho + \sigma\cos\left(\frac{\pi}{2\omega}\lambda\right)\right\}$$
$$+ \sigma\sin(\lambda\tau_1)\sin\left(\frac{\pi}{2\omega}\lambda\right) = \frac{5}{3},$$
$$\sin(\lambda\tau_1)\left\{\rho + \sigma\cos\left(\frac{\pi}{2\omega}\lambda\right)\right\}$$
$$- \sigma\cos(\lambda\tau_1)\sin\left(\frac{\pi}{2\omega}\lambda\right) = \frac{\omega - \lambda}{3\mu}. \quad (C1)$$

Squaring both sides of Eq. (C1) and summing, we obtain

$$W(\lambda) - \cos\left(\frac{\pi}{2\omega}\lambda\right) = 0, \quad (C2)$$

where

$$W(\lambda) := \frac{1}{2\rho\sigma}\left(\frac{25\mu^2 + (\omega - \lambda)^2}{9\mu^2} - \rho^2 - \sigma^2\right).$$

If there is no λ satisfying Eq. (C2), then there is no λ satisfying Eq. (9). Thus, we focus on Eq. (C2) instead of Eq. (9). Note that the sign of $W(\lambda)$ is governed by the sign of $\sigma\rho$. Here, we assume $\sigma\rho \geqslant 0$ and divide λ into two ranges: (i) $\lambda \leqslant \omega$ and (ii) $\omega \leqslant \lambda$.

For (i) $\lambda \leqslant \omega$, we define the new function

$$V(\lambda) := -\frac{\pi}{2\omega}(\lambda - \omega). \quad (C3)$$

Obviously, $V(\lambda) \geqslant \cos[\lambda\pi/(2\omega)]$ holds within range (i). The function $W(\lambda) - V(\lambda)$ is a quadratic function, which has a minimum at

$$\lambda = \lambda_c := \omega - \frac{9\pi\mu^2\rho\sigma}{2\omega}.$$

Under assumption (14), $W(\lambda_c) - V(\lambda_c) > 0$ holds. Thus, $W(\lambda) > V(\lambda) \geqslant \cos[\lambda\pi/(2\omega)]$ holds. In other words, there is no λ satisfying Eq. (C2) within range (i).

For (ii) $\omega \leqslant \lambda$, the left side of Eq. (C2) is a monotonically increasing function of λ in range (ii). Furthermore, the left-hand side of Eq. (C2) is positive for $\lambda = \omega$. Therefore, there is no λ satisfying Eq. (C2) within range (ii).

Using the same procedure, we can prove that there is no λ satisfying Eq. (C2) for $\rho\sigma < 0$. From (i) and (ii) above, there is no λ satisfying Eq. (C2) if the coupling delays τ_1 and τ_2 satisfy Eq. (18). Thus, the stability of $g(s,\rho,\sigma)$ is maintained even if τ_1 varies arbitrarily. Since the stability of $g(s,\rho,\sigma)$ is guaranteed for $\tau_1 = \pi/(2\omega)$ in Lemma 1, the proof is complete. ∎

[1] A. Pikovsky, M. Rosenblum, and J. Kurths, *Synchronization* (Cambridge University Press, Cambridge, 2001).

[2] T. Ikeguchi and I. Tokuda, Nonlin. Theor. Appl., IEICE **3**, 112 (2012).

[3] G. Saxena, A. Prasad, and R. Ramaswamy, Phys. Rep. **521**, 205 (2012).

[4] A. Koseska, E. Volkov, and J. Kurths, Phys. Rep. **531**, 173 (2013).

[5] D. Aronson, G. Ermentrout, and N. Kopell, Physica D **41**, 403 (1990).

[6] K. Bar-Eli, Physica D **14**, 242 (1985).

[7] Y. Yamaguchi and H. Shimizu, Physica D **11**, 212 (1984).

[8] D. V. Ramana Reddy, A. Sen, and G. L. Johnston, Phys. Rev. Lett. **80**, 5109 (1998).

[9] D. R. Reddy, A. Sen, and G. L. Johnston, Physica D **129**, 15 (1999).

[10] S. Strogatz, Nature (London) **394**, 316 (1998).

[11] F. M. Atay, Phys. Rev. Lett. **91**, 094101 (2003).

[12] Y. Kyrychko, K. Blyuss, and E. Schöll, Eur. Phys. J. B **84**, 307 (2011).

[13] Y. N. Kyrychko, K. B. Blyuss, and E. Schöll, Philos. Trans. R. Soc. A **371**, 20120466 (2013).

[14] K. Konishi, H. Kokame, and N. Hara, Phys. Rev. E **81**, 016201 (2010).

[15] K. Konishi, H. Kokame, and N. Hara, Phys. Lett. A **374**, 733 (2010).

[16] A. Gjurchinovski, A. Zakharova, and E. Schöll, Phys. Rev. E **89**, 032915 (2014).

[17] Y. Sugitani, K. Konishi, and N. Hara, Phys. Rev. E **92**, 042928 (2015).

[18] G. Saxena, A. Prasad, and R. Ramaswamy, Phys. Rev. E **82**, 017201 (2010).

[19] W. Zou, D. V. Senthilkumar, Y. Tang, and J. Kurths, Phys. Rev. E **86**, 036210 (2012).

[20] K. Konishi, L. Le, and N. Hara, Eur. Phys. J. B **85**, 166 (2012).

[21] W. Zou, D. V. Senthilkumar, Y. Tang, Y. Wu, J. Lu, and J. Kurths, Phys. Rev. E **88**, 032916 (2013).

[22] T. Biwa, S. Tozuka, and T. Yazaki, Phys. Rev. Appl. **3**, 034006 (2015).

[23] A. Sharma, K. Suresh, K. Thamilmaran, A. Prasad, and M. Shrimali, Nonlin. Dyn. **76**, 1797 (2014).

[24] S. R. Huddy and J. D. Skufca, IEEE Trans. Power Electron. **28**, 247 (2013).

[25] C. Cakan, J. Lehnert, and E. Schöll, Eur. Phys. J. B **87**, 54 (2014).

[26] W. Zou and M. Zhan, Phys. Rev. E **80**, 065204 (2009).

[27] R. Merris, Lin. Alg. Appl. **278**, 221 (1998).

[28] F. M. Atay and T. Bıyıkoğlu, Phys. Rev. E **72**, 016217 (2005).

[29] M. Asllani, D. Busiello, T. Carletti, D. Fanelli, and G. Planchon, Sci. Rep. **5**, 12927 (2015).

[30] C. Murguia, J. Pena, N. Jeurgens, R. H. Fey, T. Oguchi, and H. Nijmeijer, IFAC-PapersOnLine **48-18**, 245 (2015).

[31] K. Oooka and T. Oguchi, Int. J. Bifurcation Chaos **26**, 1630028 (2016).

[32] W. L. Kath and J. M. Ottino, Science **316**, 1857 (2007).

[33] I. Z. Kiss, C. G. Rusin, H. Kori, and J. L. Hudson, Science **316**, 1886 (2007).

[34] A. Zlontnik, R. Nagao, I. Z. Kiss, and J. Li, Nat. Commun. **7**, 10788 (2016).

[35] C. Bick and E. A. Martens, New J. Phys. **17**, 033030 (2015).

[36] Y. Sugitani, in *Proceedings of the Internationl Symposium on Nonlinear Theory and Its Applications* (IEICE, Tokyo, Japan, 2016), pp. 667–670.

[37] F. Atay, J. Diff. Eq. **221**, 190 (2006).

[38] P. V. Mieghem, *Graph Spectra for Complex Networks* (Cambridge University Press, Cambridge, 2012).

[39] M. Fu, A. Olbrot, and M. Polis, IEEE Trans. Autom. Control **34**, 813 (1989).

[40] K. Gu, V. L. Kharitonov, and J. Chen, *Stability of Time-delay Systems* (Springer Science, New York, 2003).

[41] K. Konishi and H. Kokame, Phys. Lett. A **366**, 585 (2007).

[42] W. Zou, D. V. Senthilkumar, M. Zhan, and J. Kurths, Phys. Rev. Lett. **111**, 014101 (2013).

[43] S. P. Bhattacharyya, A. Datta, and L. H. Keel, *Linear Control Theory: Structure, Robustness, and Optimization* (CRC, Boca Raton, FL, 2009).

[44] E. Fridman, *Introduction to Time-delay Systems* (Birkhäuser, Basel, 2014).